

Article

A Note on the Johnson–Mehl–Avrami–Kolmogorov Kinetic Model: An Attempt Aiming to Introduce Time Non-Locality

Jordan Hristov 

Department of Chemical Engineering, University of Chemical Technology and Metallurgy, 8 Kliment Ohridsky, Blvd., 1756 Sofia, Bulgaria; jordan.hristov@mail.bg or jyh@uctm.edu

Abstract: This note aims for a non-local extension of the Johnson–Mehl–Avrami–Kolmogorov (JMAK) kinetic equation, describing solid phase transformation through the implementation of the time-fractional Caputo derivative and Mittag-Leffler function instead of the exponential Avrami kinetics. These are preliminary results that include tests on some published data and a clarification of the concept.

Keywords: JMAK kinetics; crystallization; Caputo derivative; Mittag-Leffler function

1. Introduction

This note addresses a formal extension of the Johnson–Mehl–Avrami–Kolmogorov (JMAK) equation of phase transformation (crystallization) [1–5]. This equation, following Kolmogorov, can express the classical JMAK transformation theory for liquid–solid crystallization processes as [5]

$$X = 1 - \exp(X^*) \quad (1)$$

correlating the actual X and extended transformed fraction $X^* = 1 - X$ of the material with randomly distributed nuclei, moving towards the complete occupation of the space by the new phase.

For $X = 1$, the material is completely transformed. In a more frequently presented form, the JMAK equation is

$$X = 1 - \exp(-kt^n) \quad (2)$$

In (2), k (with the dimension s^{-n}) is a prefactor determined by the thermodynamic conditions, and n is the Avrami exponent. In a doubly logarithmic scale, $\ln(-\ln(1-x)) = nt$, the slope defines the Avrami exponent. As follows from Avrami theory [1–3], this exponent depends on the geometry of the crystallizing material: $n = 2$ in a linear case (as a rod or filament), $n = 3$ in a planar configuration and $n = 4$ in a three-dimensional space. Despite the simple form of (2), its parameters, specifically the exponent n , provide information about the mechanism involved in the transformation process.

The JMAK equation corresponds to an isothermal condition of transformation [6], but its applications and modifications [7–12] are widely applied to non-isothermal cases [8,9] and processes outside crystallization, such as the intercalation [13] and dehydration of minerals [14].

Despite its simplicity, the JMAK equation is under intensive study and modifications to improve its applications to cases where the integer-order Avrami exponents mentioned above are not confirmed by the data fitting procedure (see, for example, [14–16] and many others devoted to its applications). For a deep understanding of the physical mechanism driving the transformation kinetics and the basic assumption of the JMAK theories [1–5],



Academic Editor: Dimitris S. Achilias

Received: 19 December 2024

Revised: 8 January 2025

Accepted: 21 January 2025

Published: 22 January 2025

Citation: Hristov, J. A Note on the Johnson–Mehl–Avrami–Kolmogorov Kinetic Model: An Attempt Aiming to Introduce Time Non-Locality. *Eng* **2025**, *6*, 24. <https://doi.org/10.3390/eng6020024>

Copyright: © 2025 by the author. Licensee MDPI, Basel, Switzerland.

This article is an open access article distributed under the terms and conditions of the Creative Commons Attribution (CC BY) license (<https://creativecommons.org/licenses/by/4.0/>).

we refer to the excellent analysis by Cahn [17] and the book by Christian [18]; a good read is Chapter 21 of [19].

On this note, we do not intend to perform a systematic review of the JMAK-related models but focus our efforts on a non-local extension involving the time-fractional Caputo derivative applied to a modified fractional kinetic equation of the pseudo-first order, which provides a solution in terms of the Mittag-Leffler function without any attempt to revise the underlying principles of the JMAK equation's derivations.

This study is motivated by the fact that in the dynamic process of phase transformation, there is a time shift between the current state and the already-transformed (earlier) state. The general relationship between the input $x(t)$ and the output $y(t)$ of a certain dynamic system is generally described using a convolution integral relation as a general formulation of the causality principle [20,21], namely

$$y(t) = \int_0^t R(t-s)x(s)ds \quad (3)$$

where $R(t-s)$ is a correlation (memory) function relating to the recent states having a stronger effect on the current state than the far-past states of the system. For instance, some traces of this point of view can be found in the equation [1–5]

$$X = 1 - \exp(-k(t-t_0)^n) \quad (4)$$

where t_0 is the delay from the nuclei's appearance to the crystallization's onset. This equation was the starting model in Kolmogorov's solution [5], yielding (1).

Hence, we may formulate a general relationship between the rate of crystallization dX/dt and the remaining (reduced) crystallization as a convolution:

$$\frac{dX}{dt} \equiv \int_0^t R(t-s)X^*(s)ds, \quad X^* = 1 - X, \quad X(0) = 0, \quad X(\infty) = 1, \quad t > 0 \quad (5)$$

which is a formulation relevant to the Boltzmann superposition principle [22].

Formulation (5) will be developed in detail in the sequel of this note (see Sections 3.2 and 3.3).

Remark 1 (The term of memory). *It is worth stressing that the term **memory** used in the formulation of (4) does not match with the **melt memory** or **crystallization memory** widely discussed in the literature; see, for example, [23–25] and many others related to them.*

Remark 2 (Non-locality: some additional comments). *In the context of the general definition of dynamic non-locality expressed by Equation (5), we have to refer to the application of such an approach to other aspects of thermodynamic systems out of equilibria, applying either a time delay (the dual-phase lag) [26] or fractional calculus technology [27,28]. To be correct, we have to mention that the time delay [26] and the non-locality, as presented in Equation (5), are two different concepts from physical and mathematical points of view. In this way, we stress this again: time non-locality is considered and applied in this work since there is no instant phase transformation, i.e., processes with infinite speed do not exist. The time lag concept assumes a relaxation, applying the Cattaneo concept with a Taylor series expansion of the Fourier law in terms of local (integer-order) derivatives and assumed exponential memory; this leads to a hyperbolic equation. In contrast, in the non-locality expressed by a convolution, the memory function is a correlation function between the input and output of the system and cannot be erroneously considered as a time delay. However, there is a way to perform an artificial fractionalization of the model equation by replacing the integer-order Taylor series expansion with a fractional counterpart in the form of Caputo derivatives*

(as is performed in [26]); examples of such a formalistic approach are available elsewhere [29]. More details concerning the concept accepted here are available in Sections 3.2 and 3.3.

1.1. Aim

This note aims to present a new point of view of the description of the JMAK kinetic model by implementing non-locality in time using a time-fractional Caputo derivative and a general solution in terms of the Mittag-Leffler function of one parameter as a generalization of the local JMAK kinetics with exponential phase growth. The emphasis is on the formalization of the kinetic equation rather than on its derivation (beyond the scope of this communication).

1.2. Further Text Organization

The following part of this note is organized as follows. Section 2 presents the physical background of crystallization as a transformation process (Section 2.1), the case of isothermal crystallization (Section 2.1.1) and the kinetic models pertinent to it (Section 2.1.2). The new approach to a non-local extension of the JMAK model is developed in Section 3, as a formal treatment of the Avrami kinetic model (Section 3.1) and an explanation based on the causality of dynamic systems resulting in a time-fractional equation with a Caputo derivative (Section 3.3). Applications of the new approach are presented in Section 4 with the qualitative simulation of $\theta(t) = 1 - X(t)$ and $X(t)$ plots (Section 4.1) and tests on published data (Section 4.2). For concise exposition, the supporting information pertinent to the fractional Caputo derivative and the Mittag-Leffler function is summarized in Appendix A.

2. Crystallization: The Basic Features of the Process and JMAK's Formal Kinetics

Before continuing, we need to discuss a few basic characteristics of the phase transformation in connection with the JMAK kinetics.

2.1. The Physical Background

Crystallization as a process of phase transformation is commonly described by a kinetic equation describing the time extent of the degree of crystallization (the fraction of the crystallized phase), expressed in a general form as time and a time-temperature-dependent functional:

$$X = X(t, T) \quad (6)$$

$$X = \frac{M_c}{M_{p-total}} = \frac{\rho_c \sum V_j(t)}{\rho_l V_0} \quad (7)$$

with the initial condition $X(t = 0) = 0$ and $\sum V_j(t = 0)$ (the total sum of the volume with the crystallized mass). And, at $t \rightarrow \infty$, when there is only completely crystallized material, $X(\infty) = 1$ and $\sum V_j(\infty) = V_0 \frac{\rho_l}{\rho_c}$.

There are three main kinetic processes [19,30]:

- Isothermal crystallization kinetics.
- Constant cooling rate crystallization kinetics.
- Crystallization upon non-linear cooling.

We restrict ourselves to the isothermal kinetics described by the JMAK equation because the main idea is to demonstrate the application of the Mittag-Leffler function to a non-local extension of this kinetic model rather than to start modeling from first principles, which is beyond the scope of this note.

2.1.1. Isothermal Crystallization

For isothermal crystallization, when the rapid cooling of liquid polymers takes place (at temperatures T_c above their melting points), the models developed are based on the following assumptions [30]:

- The rate of temperature change is much less than the rate of thermal diffusion; that is, $dT/dt \ll (a/L^2)T$ where $a = \lambda/\rho C_p$ [m^2/s] is the thermal diffusivity, λ [W/mK] is the thermal conductivity and ρ [kg/m^3] and C_p [J/kg] are the density and heat capacity, respectively.
- The latent heat release is much lower than the heat transfer rate.
- The ratio of the densities in the crystalline and liquid phases ρ_c/ρ_l does not change and is assumed to be constant.
- The process is carried out in a finite volume and is controlled by the rate $\frac{dX}{dt} = \frac{h(T)}{g(X)}$.

Thus, the phase transformation rate depends on $h(T)$, which is only a temperature-dependent function, where $g(X)$ is a function of the transformed amount of mass. Moreover, the transformation kinetics depend on the geometrical and spatial conditions of the process of crystallized mass growth [19,30].

2.1.2. Kinetic Models

A first-order kinetic equation: [31]

$$\frac{dX}{dt} = k(t)(1 - X) \quad (8)$$

Common kinetics of nucleation and growth: [32]

$$\frac{dX}{dt} = f_{nucl}(T, X) + f_{growth}(T, X) \quad (9)$$

$$X = 1 - \frac{C_0 + 1}{C_0 + \exp[-C_1(T)t]} \quad (10)$$

with the material constants C_0 and C_1 ; for $C_0 = 0$, we get (8).

The Avrami equation of the n^{th} order [1]:

$$\frac{dX}{dt} = nkt^{-1}(1 - X) \quad (11)$$

$$X = 1 - \exp[-k(T)t^n] \quad (12)$$

$$k(T) = \frac{\alpha}{V_0} \frac{\rho_l}{\rho_c} N(T)[G(T)]^{n-1} \quad (13)$$

$k(T)$ is the temperature-dependent crystallization rate constant; $N(T)$ is the nucleation rate; and α is the geometrical constant.

The Avrami exponent n is affected by the molecular weight, nucleation type and secondary crystallization [19,30]. We will skip such details and refer to the cited literature for more information since our efforts are directed toward the formalization of the JMAK kinetics, which, as mentioned, are applied not only to the processes where they originated but to a broad range of phase change processes, such as crystallization in nanocomposites [33], solid-state reactions [34], the stability of amorphous solid dispersions [35], intercalation processes [13], fat crystallization [36,37] and the dehydration of minerals [14].

Remark 3 (The k constant). *In the original Avrami kinetics, the rate constant k has a dimension of s^{-n} , and the model has no characteristic time scale. We may present the rate constant k as $k = k_0^n \Rightarrow k_0 = k^{1/n}$, which allows the product kt^n in the original Avrami version to be presented*

as $kt^n = (k_0t)^n$. This is not strange, commonly used in the treatment of crystallization kinetic data (see, for example, [37]). If such a presentation of the product kt^n is accepted, then k_0 (a dimension of s^{-1}) can be used as a time scale. From this point of view, k_0t could be considered a pseudo-Fourier number (dimensionless time). However, the JMAK model has no time scale, and this is an open problem that should be resolved; if such a time scale exists, then with a stipulated value of n , following the JMAK theory, we should extract this by data fitting only the value of k_0 ; this is the mathematically correct approach because in the single Avrami equation, we have two unknowns to be determined, while a second equation is missing (it is artificially created as a step of the regression analysis, and this refers to its essence, which, since the massive use of computer codes, has been forgotten). Using only one equation leads to effects of n on k [38], but using $(kt)^n$ or $(k_0t)^n$, the problem can be eliminated (see the comments in [37]), despite the critiques in [39] on the approach used in [37,38], suggesting an expansion of the Avrami exponential function as a power series; we can see in the sequel that the Mittag-Leffler function works in this direction (see the comments in Section 4.1).

3. The JMAK Kinetic Model Reconsidered

3.1. A Formal Treatment of the JMAK Kinetics

Now, we will try to perform a formalization of the JMAK kinetics, envisaging an extension of their application. As a first step, let us consider Equation (11), taking into account the fact that $dX/dt = -d(1 - X)/dt$ and denoting $\theta = 1 - X$, resulting in

$$\frac{d\theta}{dt} = -knt^{n-1}\theta \tag{14}$$

Applying the non-linear transformation of the time scale as $\tau = t^n$, meaning $\ln \tau = n \ln t$, a linear relationship in a logarithmic scale, we obtain a first-order kinetic model,

$$\frac{d\theta}{d\tau} = -k\theta \tag{15}$$

with a simple solution:

$$\theta = \exp(-k\tau) = \exp(-kt^n) \Rightarrow X = 1 - \exp(-kt^n) \tag{16}$$

The formal transformation of (11)–(15) will help us to extend these non-linear kinetics to the area of non-local (fractional) modeling, as explained next.

3.2. An Extended Non-Local Presentation of the JMAK Kinetics

We start with (15), expressing it through the time-fractional Caputo derivative (see Appendix A.1.2).

$$D_t^\mu \theta = \frac{\partial^\mu \theta}{\partial \tau^\mu} = -k\theta, \quad 0 < \mu < 1, \quad t > 0 \tag{17}$$

with the solution [40]

$$\theta(\tau) = E_{\mu,1}(-k\tau^\mu) \tag{18}$$

$E_{\mu,1}(-k\tau^\mu)$ is the Mittag-Leffler function of one parameter [40] (for the properties of the Mittag-Leffler function, see Appendix A.2).

For $\mu = 1$, $E_{\mu,1}(-k\tau^\mu) \rightarrow \exp(-k\tau)$ and (17) reduces to (16).

We may present (18) in an extended form that will help us to explain what we mean by the fractional extension of the JMAK kinetic model, namely

$$\theta(\tau) = E_{\mu,1}(-k\tau^\mu) = \sum_{j=0}^{\infty} \frac{(-1)^j k^j \tau^{j\mu}}{\Gamma(j\mu + 1)} = 1 - \frac{k\tau^\mu}{\Gamma(\mu + 1)} + \frac{k^2\tau^{2\mu}}{\Gamma(2\mu + 1)} + \dots \tag{19}$$

If we consider only a limited number of terms, i.e., a truncated Mittag-Leffler function, then

$$\theta(\tau) \approx \sum_{j=0}^J \frac{(-1)^j (k\tau^{j\mu})}{\Gamma(j\mu + 1)} = 1 - \frac{k\tau^\mu}{\Gamma(\mu + 1)} + \frac{k^2\tau^{2\mu}}{\Gamma(2\mu + 1)} + \dots + \frac{k^J\tau^{J\mu}}{\Gamma(J\mu + 1)} \tag{20}$$

Now, in terms of the time, we have the relation $\tau = t^n$, which can simply be inserted in (19) with the simple assumption that n depends only on the geometry of the crystallizing system: $n = 2$ for a linear system, $n = 3$ for a plate-like system and $n = 4$ in the case of a spherical system.

Therefore, we focus on the value of the fractional order $0 \leq \mu \leq 1$ and the number of terms in the truncated Mittag-Leffler function.

3.3. Explanations Concerning the Non-Local Approach

We now attempt to explain the transition from local to non-local kinetics concisely. For example, as stated in the previous section and textbooks, kinetic equations in chemical kinetics are often local, or memoryless. For instance, the first-order local kinetic equation of $N(t)$ is

$$\frac{d}{dt}N(t) = -c_0N(t), \quad c_0 > 0, \quad N_0 = N(t = 0) \tag{21}$$

where c_0 is a prefactor, and it has the solution

$$\int_0^t \frac{dN(t)}{N(t)} dt = - \int_0^t c_0 dt \Rightarrow N(t) = N_0 \exp(-c_0 t) \tag{22}$$

Since no dynamic process can operate at infinite speeds, the realistic perspective that there are temporal delays between the causes (reasons) and the results (reactions) naturally leads to non-locality. With the concept of causality, the reaction (or output) cannot come before the cause. This can be presented in a simplified form of (1) relating the rate dN/dt of the changing value $N(t)$ characterizing the dynamic system to its past values over the time interval $t - s$ through the functional differential equation

$$\frac{dN}{dt} = -c \int_0^t R(t-s)N(s) d\tau \tag{23}$$

Here, $R(t - \tau)$ is the correlation function (memory kernel) relating the current version of N to its past values over the time interval s ; its closest values have stronger contributions than the oldest ones. The general condition in this non-local functional relationship conveying the causality principle [20,21] is that $R(t)$ should be a causal function, and the integral in (23) is a convolution integral; since t represents the processing time (i.e., the process duration), rather than a time instant, $R(t)$ should be monotonically declining and vanishing for $t \rightarrow \infty$ and negligible (i.e., equal to zero) for $t < 0$ [41]. If the initial value of N_0 at $t = 0$ is non-zero, then this should be taken into account.

Let us consider (21) again and integrate it, but present it in a general manner, the way in which it was considered in [42].

$$N(t) = N_0 - c_0 D_t^{-1} N(t) \tag{24}$$

with ${}_0D_t^{-1}$ denoting the standard Riemann integral, the same integral that in (22) yields the exponential function. Then, the introduction of non-locality can be performed by replacing only ${}_0D_t^{-1}$ with ${}_0D_t^{-\mu}$ where $0 < \mu < 1$ in (24). The final result is [42]

$$N(t) = N_0f(t) - c_0D_t^{-\mu}N(t) \tag{25}$$

In the case of the non-local kinetics of the first order, with a zero initial condition ($N_0 = 0$), that is, no crystals exist at $t = 0$, we have

$$N(t) = -c_0D_t^{-\mu}N(t) \tag{26}$$

This approach can be simply explained by the convolution relationship

$$N(t) = -c_\mu D_t^\mu N(t) = -c_\mu I^\mu N(t) = \frac{1}{\Gamma(\mu)} \int_0^t \frac{N(s)}{(t-s)^\mu} ds \tag{27}$$

where $D_t^{-\mu}N(t) = I^\mu N(t)$ is the Riemann–Liouville fractional integral with a memory function, $\frac{t^{-\mu}}{\Gamma(\mu)}$.

Now, applying the Caputo derivative D_t^μ to both sides of (27), we obtain

$$D_t^\mu N(t) = -c_\mu N(t) \Rightarrow N(t) = E_\mu(-c_\mu t^\mu) \tag{28}$$

Power law memory is a special case coming from classical fractional calculus [43], and we use it to explain more familiarly the transition from local to non-local kinetics when the JMAK model is considered and the Mittag-Leffler function is used instead of the Avrami exponential relationship. This does not restrict the application of the general formulations (24) and (25), where the memory function could be of a different kind directly related to the physics of the described process; more examples of non-local kinetics are available elsewhere [44].

4. The Application of the New Approach

4.1. Qualitative Plots of $\theta(t)$ and $X(t)$

Before performing any test on real data, we had to see what the behavior of the Mittag-Leffler function was when direct calculations were applied as a series. This step focused on three points: (1) Does the directly simulated series have behaviors qualitatively mimicking the real plot? (2) What is the minimum number of terms in the series ensuring stable calculations? (3) What is the upper limit of terms allowing for rational calculations?

Qualitative plots of $\theta(t)$ and $X(t)$ calculated directly with the Mittag-Leffler function as a series (50 terms in Maple) are shown in Figure 1. These plots only demonstrate the suitability of the new approximations. Moreover, the tests revealed that with less than 25 terms in the series, the calculations were unstable (see the examples in Figure 2), and because of that, the simulations presented further in this study were obtained with a minimum of 50 terms in the Mittag-Leffler series. The upper limit of terms in the series used in this study was about 180, but this is a problem for a separate investigation beyond the scope of this work.

We already commented on the exponent k in Remark 3, but now we have to emphasize its important role in the time range of plot simulations. The first question that comes to mind when seeing the plots in Figure 1 is why the time range is so large when we know that the Mittag-Leffler function can only be calculated as a series for small arguments. The answer to this question lies in the value of k . For the cases with $n = 2$, $n = 3$ and $n = 4$, we had an average value of $k = 2.5 \cdot 10^{-7}$ (for sporadic nucleation) [37], while in case (a),

$k = 8 \cdot 10^{-11}$ (instantaneous nucleation) [37]. Regarding the product kt^n , we can see that in the case of (a), kt^n_{max} was approximately $kt^n_{max} \approx 1.37 \cdot 10^{-4}$, while for cases (b), (c) and (d) with $k = 2.5 \cdot 10^{-7}$, we had $kt^2_{max} \approx 5 \cdot 10^{-4}$, $kt^3_{max} \approx 3 \cdot 10^4$ and $kt^4_{max} \approx 6.25 \cdot 10^{-4}$; there are many data leading to such results in the references quoted in this article. Thus, denoting $y = kt^n$, we obtain $E_\mu(-y^\mu)$ with arguments less than 1, approaching the Mainardi asymptotic for t_{0+} , and this allows us to calculate $\theta(t) = E_\mu(-y^\mu)$ and $X(t) = 1 - \theta(t)$ directly as a series.

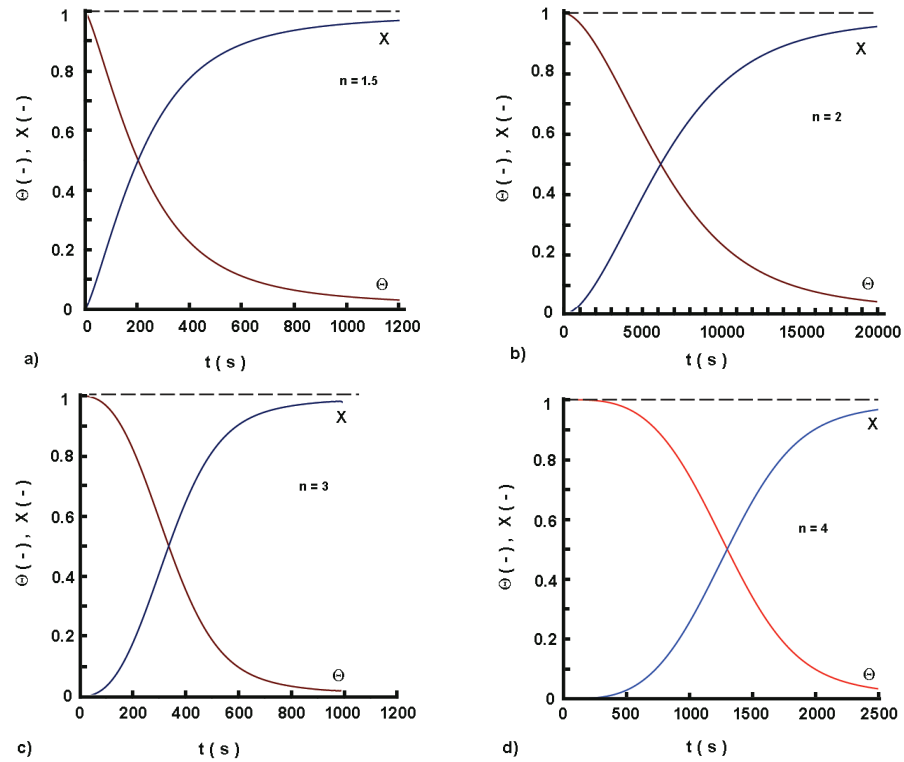


Figure 1. Qualitative plots of $\theta(t)$, left column, and $x(t)$, right column, for the stipulated values of the exponent n (taken from [37]): $k = 8 \cdot 10^{-4}$ for (a); $k = 2.5 \cdot 10^{-7}$ for (b–d). For all cases, $\mu = 0.85$, and there were 80 terms in the series.

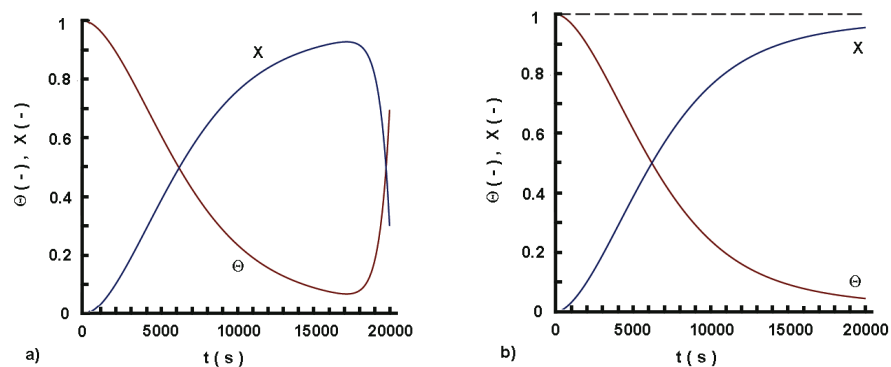


Figure 2. Qualitative plots of $\theta(t)$ and $X(t)$ for stipulated values of the exponent $n = 2$, showing the effect of a low number of terms (18) (panel a) and a high number of terms in the series (180) (panel b)). For all cases, $\mu = 0.85$ and $k = 5.5 \cdot 10^{-7}$ (taken from [37]).

4.1.1. Qualitative Plots of $\theta(t)$ and $X(t)$ and Dimensionless Time

The preceding comments on the value and effect of the Avrami constant provoked an idea that we would like to express briefly since it is directly related to the application of the Mittag-Leffler series as an approximating function.

The original Avrami product kt^n is dimensionless and, as we commented above, can be used as the approximation of arguments in the Mittag-Leffler series. Now, let us suggest that $k = k_0^n$, such that $k_0 = k^{1/n}$, as was mentioned in Remark 3. This substitution allows the product kt^n to be presented as $kt^n = (k_0t)^n$. Then, since k_0 has a dimension inverse to time but is only temperature-dependent, following the JMAK theory, we may suggest that the characteristic time scale is $t_0 = 1/(1/k_0)$, such that the product $Y = k_0t$, an analog of the diffusional Fourier number, is the dimensionless time. With this step, we may express our approximations through the Mittag-Leffler functions as $E_\mu(-(k_0t)^{n\mu}) = E_\mu(-Y^{n\mu})$ with $n = 1, 2, 3$ or 4 , respectively, depending on the transformation process considered. We have an ongoing kinetic process happening in a time less than the characteristic time scale when $0 \leq Y \leq 1$.

Now, as a numerical experiment, in Figure 3, we repeat the simulations from Figure 1, with $n = 3$ as an example, but with Y as the time scale and various values of the fractional order μ .

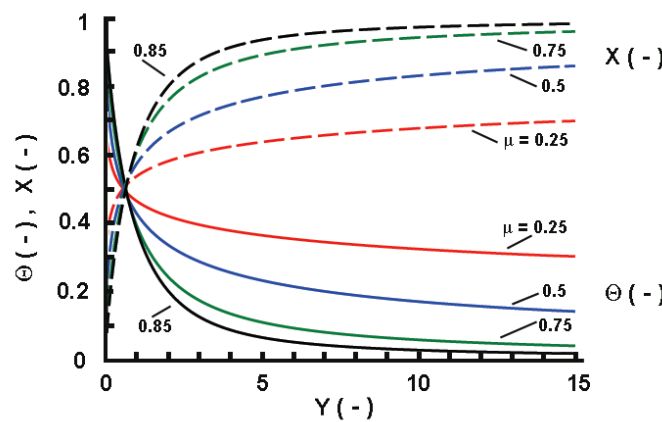


Figure 3. Qualitative plot of $\theta(t)$ and $x(t)$ for $n = 3$ and $k = 2.5 \cdot 10^{-7}$ against the dimensionless time Y , showing the effect of the fractional order μ as a rate-controlling parameter.

The plot in Figure 3 reveals that the fractional order μ controls the behavior of the curves. Thus, with the stipulated value of k , k_0 and n , the fractional order μ is a new parameter that can characterize the phase transition behavior.

Remark 4 (The time scale definition). *It is worth stressing that the time scale should be defined before the experiment, as was performed with k_0 , but not after its completion. We emphasize this definition because if the time for the complete phase transformation is taken as a time scale, as one might expect, then we may again define a dimensionless time varying between 0 and 1. However, its definition would be incorrect because all scales related to the length, time, mass or any other varying process variables should be defined before the experiment based on process parameters that do not vary with them is carried out; in the case of an isothermal transformation, k (or k_0) is time-independent and depends only on the imposed thermal conditions.*

The last statement in Remark 4 is relevant to the comments in Remark 3 that with one equation, two parameters cannot be determined correctly because they become interrelated; k should be defined based on thermodynamic considerations, and then the Avrami exponent n can be determined correctly from the exponential relationship. In the concept explored in this note, both k and n are stipulated based on the thermal conditions and suggested spatial transformation evolution, but a new parameter that should account for any deviations from the perfect conditions is the fractional parameter $0 \leq \mu \leq 1$; this is beyond the scope of this work, but the idea is worthy to be explored.

4.1.2. Estimation of Fractional Order μ : Initial Steps

Here, we suggest a pragmatic approach to the determination of μ based on Mainardi asymptotics. Taking data from experiments or tabulated from the literature, the first step was to rescale the time as $\tau = t^n$, where n is stipulated and depends on the geometry of the studied crystallizing system. Then, from asymptotic (A5), we have in a logarithmic scale

$$\ln E_\mu(-\tau^\mu) \sim \ln \left[\exp \left(-\frac{\tau^\mu}{\Gamma(1+\mu)} \right) \right] \Rightarrow \ln E_\mu(-\tau^\mu) \sim -\frac{\tau^\mu}{\Gamma(1+\mu)} \quad (29)$$

Hence, for short times, we have the approximation

$$\ln \theta_{\tau^{0+}} \sim -\frac{\tau^\mu}{\Gamma(1+\mu)} \Rightarrow \ln(-\ln \theta_{\tau^{0+}}) = \ln(-\ln(1-X)_{\tau^{0+}}) \sim -\ln \tau^\mu - \ln \Gamma(1+\mu) \quad (30)$$

That is, taking the data for short times, where the plot of θ seems to be well approximated by a power law, we may calculate in a doubly logarithmic scale the value of μ as the slope of the linear plot; this approach, to some extent, matches the technique for the determination of the Avrami exponent n .

For a long time, asymptotic (A11) provides

$$E_\mu(-\tau^\mu) \sim \frac{\tau^{-\mu}}{\Gamma(1-\mu)} \Rightarrow \ln E_\mu(-\tau^\mu) \sim \ln \left(\frac{\tau^{-\mu}}{\Gamma(1-\mu)} \right) \Rightarrow \ln \theta \sim -\mu \ln \tau - \ln \Gamma(1-\mu) \quad (31)$$

That is, having the experimental points $\theta = 1 - X$, $0 < \theta < 1$ and thus $\ln \theta < 0$, we obtain $-\ln \theta \sim \mu \ln t + \ln \Gamma(1-\mu)$, which allows us to easily find μ as the slope of the plot.

4.2. Tests on Published Data

Next, we applied the Mittag-Leffler approximation to real published data. The data points fitted by our approximation were taken using digitization from figures in the quoted literature sources. This process, to some extent, may have introduced errors since tabulated data about $X(t)$ were missing, but the most important issue at this point in time was to see if the new approach worked or not.

Note: Before describing the testing of the approximations on real data, two important facts concerning their sources and the consequent calculations have to be highlighted:

- It is worth noting that there were two types of published data, mainly presented as plots: (1) data where there were points reaching about a 100% transformation, and the fitting curves plateaued when $X \rightarrow 1$, and (2) data with an incomplete transformation where the points reached a plateau at levels of $X_{sat} < 100\%$. We describe how these cases were tested separately with the new approximation next.
- The present study focused on the fact that all parameters were in SI units. However, the published data did not always follow these rules: there were cases where the time was in hours and then k was in h^{-n} , or the time was in minutes and then k was in h^{-min} . The general rule followed in the calculations was that there was no need to transform the units into SI because the product kt^n (also k_0t) is dimensionless and, thus, it does not affect the calculation of the Mittag-Leffler function. In the following description of the tests on published data, the time axes of the plots are preserved (expressed in the original time units as published) because k , for instance, is directly related to the time units used.

4.2.1. Tests on Data Related to Complete Transformation ($X_{sat} \approx 100\%$)

As the first example, we refer to the results from [16] on the crystallization kinetics of poly(ethylene terephthalate) (PET) at different temperatures. The first plot in Figure 4 (panel a) demonstrates the effect of the fractional order μ on the successful data fitting

when both n and k were stipulated (based on preliminary considerations about n and thermodynamic calculations for k). In this example, $n = 3$ was considered instead of $n = 2.6$, determined through regression data fitting utilizing the original Avrami exponential (see Table 1 in [16]).

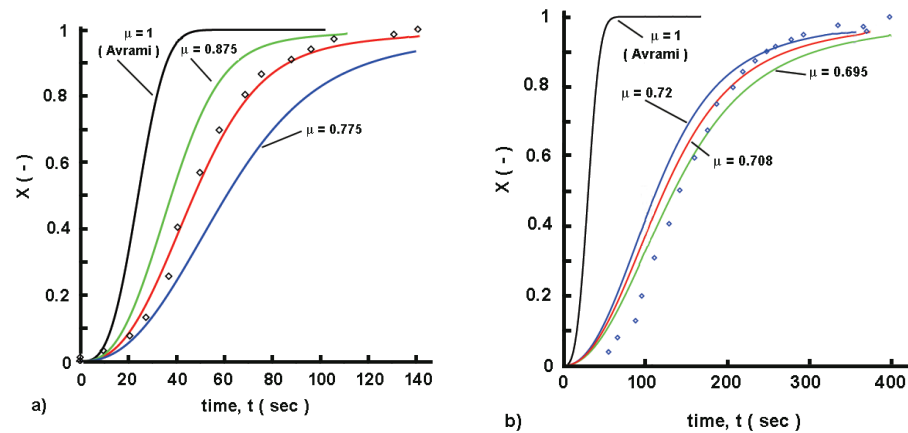


Figure 4. Test on published data with 100% transformation of poly(ethylene terephtalate) (PET) (the diamonds are the experimental points, and the same is used in the following figures). Data from [16]. (a) From Figure 1 in [16] (reduced crystallinity of PET at 180 °C). Best fit with $\mu = 0.825$. (b) From Figure 1 in [16]: case at 210 °C. Note: In all cases, $n = 3$ and $k = 2.63 \cdot 10^{-7} \text{ s}^{-1}$, and there were 80 terms in the Mittag-Leffler series.

The second test was with data from [15] concerning the crystallization of filled poly(ethylene terephtalate) ($PET - TiO_2 - 1 - 1$), shown in Figure 5.

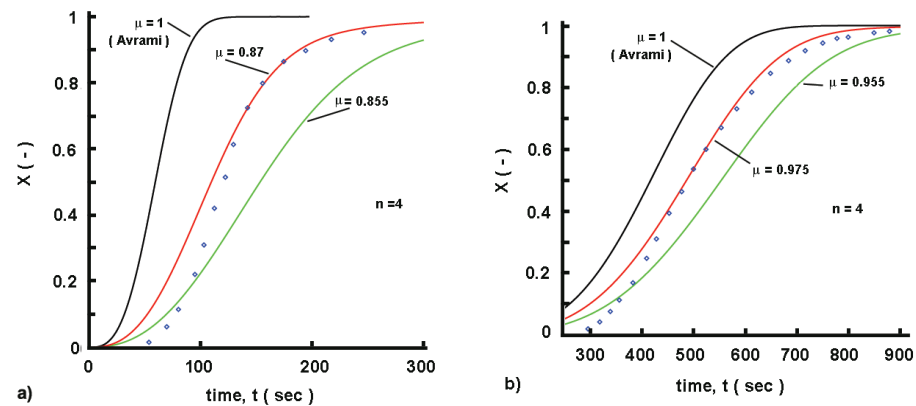


Figure 5. Test on published data with 100% transformation of filled poly(ethylene terephtalate) ($PET - TiO_2 - 1 - 1$). Data from Figure 2 in [15]. (a) Reduced crystallinity, $X(t)$, at 218 °C: $n = 4(3.5)$, $k = 2.4 \cdot 10^{-8}$. Best fit with $\mu = 0.87$. (b) Case at 224 °C: $n = 4(3.8)$, $k = 2.3 \cdot 10^{-11}$. Note: Values of n in parentheses were taken from Table 2 in [15] and determined using Avrami exponential equation. For all situations, 80 terms were used in Mittag-Leffler series.

In both tests, we could see satisfactory curves in the approximation plots through the points for medium and long times. For short times, the discrepancies could be attributed to either inexact data recovery through digitization or something that should be improved in the approximation technique; for now, this problem is open and not resolved.

Moreover, we can see how realistic the approximation was concerning the fractional order μ in Figure 4 (panel b) and Figure 5 (panel b). Specifically, for $\mu = 1$, we obtained the Avrami exponential relationship, and in Figure 5 (panel b), we see that it could not approximate the experimental points. In this context, in the data from Cheng and Shanks [15], there was a case in which the Avrami formula could not fit the data (see Figure 8 in [15]).

The fact that there was a satisfactory approximation of the data points for long times reveals that the idea conceived earlier of the preliminary estimation of the fractional order μ can be realized using the Mainardi power law asymptotic (A10) for $t \rightarrow \infty$.

Remark 5 (Why there is a discrepancy with the exponential Avrami model?). We see that there is a discrepancy between the experimental points and data fitting with the Mittag-Leffler function and the Avrami equation (the case with $\mu = 1$), and we are obliged to explain why this happens. The origin of this was commented on earlier in Remark 3. Now, we will explain this concisely. The dominating approach in the literature is the “blind” application of the least squares regression analysis of data points, either using computer codes or graphically in logarithmic coordinates. However, as mentioned in Remark 3, this an erroneous approach because following the Avrami theory, both k and n are predetermined (before the crystallization experiment), k from the thermodynamics and n from the geometry of the crystallization pattern, and there is no room to find a new process parameter controlling the correct data fitting. The regression procedure provides values of k and n that are interrelated since it does not take into account their physical meaning and the process background. As mentioned in Remark 3, it is incorrect to define two unknowns from one equation; the argument (the independent variable) is only the time t . In contrast, the new non-local approach introduces a new parameter, i.e., the fractional order μ , which allows us, along with the predetermined k and n , to control the data fitting. Moreover, it is noteworthy that in the Mittag-Leffler function generated by the new model, the argument (the independent variable) is the dimensionless product kt^n , which contrasts with the existing literature approach to the Avrami equation. From our point of view, this is an innovation simultaneously obeying the rules of thermodynamics, physics (a non-local process with a finite speed) and mathematical modeling concerning data fitting.

4.2.2. Tests on Data Related to Incomplete Transformation ($X_{sat} < 100\%$)

In cases when the entire volume is not transformed and the experimental points $X_{exp}(t)$ reach a plateau at a value of X_{sat} less than 100%, then there are two options: (1) all the data are reduced to $x = X_{exp}/X_{sat}$ so that $0 < x < 1$, and then the fitting is performed with $x = (1 - \theta(t))$ as in the case with complete transformation; (2) there is no need for the experimental point to be reduced, but the calculation should be performed through the multiplication of $X(t)$ by X_{sat} . The two examples in Figure 6 show the same behavior for the approximation lines as in the cases of complete transformation. The technique of applying the factor X_{sat} to the approximation function works acceptably, and any discrepancies can be attributed to the exactness of the digitization of the plots.

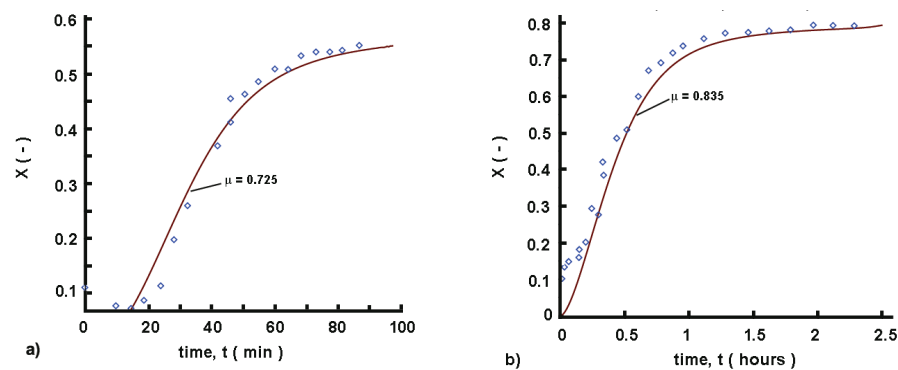


Figure 6. Test on published data with less than 100% transformations. (a) Data from Marangoni (from Figure 1 in [39]) concerning isothermal transformation of palm oil with $k = 2.53 \text{ min}^{-n}$, $n = 3$ and $X_{sat} = 0.561$. (b) From Figure 1 in [45]: isothermal cocoa butter crystallization at 19°C with $k = 3 \text{ h}^{-n}$ (from Figure 6 in [45]), $n = 2$ and $X_{sat} = 0.791$. Note: In all cases, there were 80 terms in Mittag-Leffler series.

4.3. Some Remarks on Data Simulation Using the Mittag-Leffler Function

The demonstrated data approximations (not data fitting) are tentative, showing only that the new approach works. However, for the next steps, beyond the scope of this note, reliable algorithms for data fitting specifically addressing the value of μ (because n and k are predetermined) are highly required. For now, there have been several works [46–49] applying the Mittag-Leffler function for data fitting with existing codes (starting with [46]) that might be a useful basis for creating a code specific to the JMAK model and its versions.

5. An Outline of the Results Obtained

This note only suggests the idea that the Avrami exponential equation, based on a non-linear local kinetic equation of the pseudo-first order, with the addition of simple time scaling, $\tau = t^n$, can be easily transformed into a well-known first-order kinetic model. This step, and the fact that the Mittag-Leffler function reduces to a simple exponential function when the fractional order equals unity, as well as that the time-fractional kinetic model with the Caputo derivative is a generalization of the local kinetics, allowed for a non-locality to simply be incorporated in the JMAK model.

This note uses the concept that the Avrami kinetics constant k should be calculated prior to simulations, when the exponential JMAK model is applied, to determine the exponent n , because only one equation exists with two unknowns and a second one is missing. With the extension, i.e., the fractional kinetics, resulting in the Mittag-Leffler function as an approximation, both k and n can be stipulated. A new parameter that can control the approximation and be used for the characterization of the transformation process is the fractional order μ . It is possible to perform a preliminary test with the Avrami model to see what the value of n (commonly a non-integer) is and to choose the closest integer, as we did in the test on the published data.

A non-local extension of the JMAK model is a new idea, to our knowledge never conceived of before, but it is in agreement with the concept that there is no intrinsic transformation, i.e., a transformation with infinite speed, and that crystallization could be considered as a hereditary process. Despite the fact that such a non-local extension was made with the final result of the Avrami model, it provokes a deeper exploration into its basic considerations (and of any related JMAK modifications), looking for a way for the non-locality to be implemented in the first steps of the model's construction.

To some extent, the new model and the approximating function confirm the idea of Khanna and Taylor [38] and the models of Foubert et al. [37,45] (with data tested here) that the product kt should be considered as one dimensionless variable; this was also confirmed by the test on the Marangoni data [39], even though he tried to demonstrate that this was wrong.

There have been attempts to approximate the transformation points using the high-order polynomials of power laws, as demonstrated by Marangoni in [39]. Such an approach, when the terms are power laws, $P_i t_i^p$, gives their factors (coefficients) dimensions of $time^{-p}$, which is hard to explain physically. In contrast to ad hoc polynomial approximations, all coefficients of the Mittag-Leffler function (in a truncated version considered as a polynomial) are dimensionless; this is because the variable is the product kt^n , which is also dimensionless, as was demonstrated in this note.

Probably, the text of this note will provoke many questions because it is at the interface of material science (the kinetics of materials as defined by Cantor [6]) and non-local mathematical modeling, but such an amalgamation, at the very beginning of its application, promises to be fruitful, even though some problems should be resolved (see the next section).

6. Emerging Problems That Should Be Resolved

In developing this note and the non-local version of Avrami kinetics, some problems appeared, among which were the following:

- There are not enough numerical data to allow us to test the new approximation. Dominating the literature are graphical presentations with not enough points that, even if they are presented as numerical data, are not enough to make a successful estimation of the parameters of the approximating function.
- There is a need for a code for data fitting based on the Mittag-Leffler function and specially adapted to the JMAK basic model and any of its versions to be developed; in this direction, the existing approaches and the related codes commented on in Section 4.3 would be a good basis for this to be performed.

7. Conclusions

The concept of a non-local JMAK kinetic was conceived, which resulted in the use of the Mittag-Leffler function with one parameter instead of the exponential Avrami's model. The idea was presented step by step through a non-linear scaling transform of the Avrami first-order non-linear equation and its extension as a non-local kinetic with the Caputo time-fractional derivative. Tests on published data confirmed the idea of fitting transformation data with the Mittag-Leffler function as an important role of the fractional order. The main results and problems needing to be resolved were outlined.

Funding: This research received no external funding.

Institutional Review Board Statement: Not applicable.

Informed Consent Statement: Not applicable.

Data Availability Statement: The original contributions presented in this study are included in the article. Further inquiries can be directed to the author.

Conflicts of Interest: The author declares no conflicts of interest.

Appendix A. Necessary Information Concerning the Fractional Calculus Used

This is the minimal required information concerning fractional derivatives and the Mittag-Leffler function permitting us to understand the main idea of the article.

Appendix A.1. Time-Fractional Integral and Derivatives

Appendix A.1.1. Fractional Integral

Following the Riemann–Liouville approach to fractional calculus, the fractional integral of the order $\mu > 0$ is a natural result of Cauchy's formula reducing calculations of the m -fold primitive of a function $f(t)$ to a single integral of a convolution type [40].

$${}_0I^n f(t) := f_n(t) = \frac{1}{(n-1)!} \int_0^t (t-\tau)^{n-1} f(\tau) d\tau, \quad t > 0, \quad n \in \mathbb{N} \quad (\text{A1})$$

where \mathbb{N} is a set of positive integers, and $f_n(t)$ and its derivatives of the order $1, 2, \dots, n-1$ vanish for $t < 0$. Taking into account that $(n-1)! = \Gamma(n)$, then for arbitrary positive numbers $\mu > 0$, the fractional integral of the order $\mu > 0$ is defined as

$${}_0I^\mu f(t) := \frac{1}{\Gamma(\mu)} \int_0^t (t-\tau)^{\mu-1} f(\tau) d\tau, \quad t > 0, \quad n \in \mathbb{R}^+ \quad (\text{A2})$$

For the sake of convenience, we will use also the notation ${}_0D^{-\mu}f(t)$ for ${}_0I^\mu f(t)$. Further, the law of exponents for fractional integrals means ${}_0D^{-\mu}{}_0D^{-\gamma}f(t) = {}_0D^{-\mu-\gamma}f(t) = {}_0D^{-\gamma}{}_0D^{-\mu}f(t)$.

Appendix A.1.2. Caputo Derivative

The Caputo derivative of a casual function, $f(t)$, i.e., $f(t) = 0$ for $t < 0$, is defined [40] as

$${}_CD_t^\mu f(t) = {}_0I^{1-\mu} \frac{d}{dt} f(t) = {}_0D_t^{-(1-\mu)} f^{(1)}(t) = \frac{1}{\Gamma(1-\mu)} \int_0^t \frac{f^{(1)}(\tau)}{(\tau-t)^{\mu}} d\tau \tag{A3}$$

where $0 < \mu < 1$.

The Laplace transform of the Caputo derivative is

$$L[{}_CD_t^\mu f(t);s] = s^\mu F(s) - \sum_{k=0}^{m-1} f^{(k)}(0) s^{\mu-k-1} \tag{A4}$$

The Caputo derivative of a constant is zero, i.e., ${}_CD_t^\mu C = 0$; this is consistent with what we already know about integer-order calculus.

Appendix A.2. Mittag-Leffler Function: Properties

Appendix A.2.1. Definitions

The two parameters of a Mittag-Leffler-type function are defined as a series expansion [40]:

$$E_{\mu,\beta}(z) = \sum_{k=0}^{\infty} \frac{z^k}{\Gamma(\alpha k + \beta)}, \quad \alpha > 0, \quad \beta > 0 \tag{A5}$$

When $z = \lambda t^\mu$, then

$$E_{\mu,\beta}(\pm \lambda t^\mu) = \sum_{k=0}^{\infty} \frac{(\pm 1)^k (\lambda t^\mu)^k}{\Gamma(\alpha k + \beta)} \tag{A6}$$

It is an entire function of the variable z for any $\mu, \beta \in \mathbb{C}$ or $\text{Re}(\mu > 0)$ of the order $\rho = 1/\mu$ and converges for each finite z , and therefore its sum is an analytic function in the whole complex plane. From this definition, it follows that for $\mu = 1$ and $\beta = 1$, we have

$$E_{1,1}(z) = \sum_{k=0}^{\infty} \frac{z^k}{\Gamma(k+1)} = \sum_{k=0}^{\infty} \frac{z^k}{k!} = e^z \tag{A7}$$

$$E_{1,2} = \sum_{k=0}^{\infty} \frac{z^k}{\Gamma(k+2)} = \sum_{k=0}^{\infty} \frac{z^k}{(k+1)!} = \frac{1}{z} \sum_{k=0}^{\infty} \frac{z^{k+1}}{(k+1)!} = \frac{e^z - 1}{z} \tag{A8}$$

Appendix A.2.2. Asymptotics

There are two common asymptotic approximations relevant to the present study, known as Mainardi’s conjectures, specifically a stretched exponential (the Kohlraush function) for t_{0+} and a power law for $t \rightarrow \infty$, as follows [50]:

$$E_\mu(-t^\mu) = 1 - \frac{t^\mu}{\Gamma(1+\mu)} + \dots \sim \exp\left[-\frac{t^\mu}{\Gamma(1+\mu)}\right], \quad t \rightarrow 0 \tag{A9}$$

$$E_\mu(-t^\mu) \sim \sum (-1)^{j-1} - \frac{t^{-\mu j}}{\Gamma(1-\mu j)}, t \rightarrow \infty \tag{A10}$$

and the first-order approximation of (A10) is

$$E_{\mu}(-t^{\mu}) \sim \frac{t^{-\mu}}{\Gamma(1-\mu)}, \quad t \rightarrow \infty \quad (\text{A11})$$

These approximations were tested numerically by Concezzi and Spigler [51] using the Diethelm predictor–corrector algorithm [52].

Appendix A.2.3. Calculations

The calculation of the Mittag-Leffler function is a challenging task. There are several approaches to finding suitable numerical methods, as mentioned above [51–58], with advanced techniques resolving particular cases and clarifying emerging calculation problems. For example, for a small argument, a Taylor series, spectral integral representations for intermediate values and asymptotic values for large magnitudes were used in [53]. Seybod and Hilfer [54] applied the Hankel integral representation, while Garrappa [57] applied a numerical inversion of the Laplace transform.

In the context of the task of the present article, where the analytical calculation is in the form (19) or (20), we refer to the work of Liemert and Kielne [58], where for a small and moderate argument (time), direct calculations as the series (A5) or (A6) were applied (called the direct computation of the ML series [59]), while for large arguments, the following series was used.

$$E_{\mu}(-x) = -\frac{1}{\pi} \sum_{k=1}^{\infty} (-x)^{-k} \Gamma(k\mu) \sin(k\mu\pi) \quad (\text{A12})$$

Thus, it is hard to find the right method, and the choice of which approach to use strongly depends on specific problems caused by the inclusion of the Mittag-Leffler function; in this case, a matter of argument as to what is a small argument and what is a large argument and how many terms have to be used in the direct series calculations.

References

- Avrami, M. Kinetics of phase change I: General theory. *J. Chem Phys.* **1939**, *7*, 1103–1112. [\[CrossRef\]](#)
- Avrami, M. Kinetics of phase change I: Transformation-time relations for random distribution of nuclei. *J. Chem Phys.* **1940**, *8*, 212–224. [\[CrossRef\]](#)
- Avrami, M. Kinetics of phase change I: Granulation, phase change, and microstructure. *J. Chem Phys.* **1941**, *9*, 177–184. [\[CrossRef\]](#)
- Johnson, W.A.; Mehl, R.F. Reaction kinetics in processes of nucleation and growth. *Trans. Am. Inst. Mining* **1939**, *135*, 416–458.
- Kolmogorov, A.N. A statistical theory for the recrystallization of metals. *Rep. USSR Acad. Sci. Mater. Ser.* **1937**, *3*, 355–359.
- Cantor, B. *The Equations of Materials*; Oxford University Press: Oxford, UK, 2020. [\[CrossRef\]](#)
- Blazquez, J.S.; Romero, F.J.; Conde, C.F.; Conde, A. A review of different models derived from classical Kolmogorov, Johnson and Mehl, and Avrami (KKMA) theory to recover physical meaning in solid-state transformations. *Phys. Status Solidi* **2022**, *259*, 2100524. [\[CrossRef\]](#)
- Woldt, E. The relationship between isothermal and non-isothermal description of Johnson-Mehl-Avrami-Kolmogorov kinetics. *J. Phys. Chem. Solids* **1992**, *53*, 521–527. [\[CrossRef\]](#)
- Ruitenbergh, G.; Wold, E.; Petford-Long, A.K. Comparing the Johnson-Mehl-Avrami-Kolmogorov equations for isothermal and linear heating conditions. *Thermochim. Acta* **2001**, 97–105. [\[CrossRef\]](#)
- Kourditou, D.; Chrissafis, K. Nonisothermal crystallization kinetics: Studying the validity of different Johnson-Mehl-Avrami-Erofeev-Kolmogorov (JMAEK) based equations. *Thermochim. Acta* **2021**, *704*, 179030. [\[CrossRef\]](#)
- Vazquez, J.; Lopez-Aleman, P.L.; Villares, P.; Jimenez-Garay, R. Generalization of the Avrami equation for the analysis of non-isothermal transformation kinetics. Application to the crystallization of the Cu_{0.20}As_{0.30}Se_{0.50} alloy. *J. Phys. Chem. Solids* **2000**, *61*, 493–500. [\[CrossRef\]](#)
- Tomellini, M. Kolmogorov-Johnson-Mehl-Avrami kinetics for non-isothermal phase transformations ruled by diffusional growth. *J. Therm. Anal. Calorim.* **2014**, *116*, 853–864. [\[CrossRef\]](#)
- Benes, L.; Zima, V.; Budysova, I.; Votinsky, J. A kinetic study of the intercalation of ethanol into vanadyl phosphate. *J. Incl. Phenom. Mol. Recogn. Chem.* **1996**, *26*, 311–319. [\[CrossRef\]](#)
- Bray, H.J.; Redfern, S.A.T. Kinetics of dehydration of Ca-montmorillonite. *Phys. Chem. Min.* **1999**, *26*, 591–600. [\[CrossRef\]](#)

15. Cheng, S.; Shanks, R.A. The crystallization kinetics of filled poly(ethylene terephthalate). *J. Appl. Polym. Sci.* **1993**, *47*, 2149–2160. [[CrossRef](#)]
16. Kim, S.H.; Park, S.W.; Gil, E.S. Crystallization kinetic study of poly(ethylene terephthalate) with thermophoric liquid crystalline polymer blends. *J. Appl. Polym. Sci.* **1998**, *67*, 1383–1392. [8<1383::AID-APP4>3.0.CO;2-A](#). [[CrossRef](#)]
17. Cahn, J.W. The time cone method for nucleation and growth kinetics on a finite domain. *MRS Online Proc. Libr.* **1995**, *398*, 425–437. [[CrossRef](#)]
18. Christian, J.W. *The Theory of Transformations in Metals and Alloys*; Elsevier: Amsterdam, The Netherlands, 2002. [[CrossRef](#)]
19. Balluffi, R.W.; Allen, S.M.; Carter, W.C. *Kinetics of Materials*; Wiley Interscience: Hoboken, NJ, USA, 2005.
20. Mittelstaedt, P.; Weingartner, P.A. *Laws of Nature*; Springer: Berlin/Heidelberg, Germany, 2005.
21. Nussenzveig, H. *Causality and Dispersion Relations*; Mathematics in Science and Engineering; Academic Press: New York, NY, USA, 1972; Volume 95.
22. Boltzmann, L. Zur Theorie der Elastischen Nachwirkung. *Sitzungsber. Akad. Wiss. Wien. Mathem.-Naturwiss* **1874**, *70*, 275–300.
23. Ziabicki, A.; Alfonso, G.C. Memory effects in isothermal crystallization. I. Theory. *Colloid Poly. Sci.* **1994**, *272*, 1027–1042. [[CrossRef](#)]
24. Alfonso, G.C.; Ziabicki, A. Memory effects in isothermal crystallization. II. Isotactic polypropylene. *Colloid Poly. Sci.* **1995**, *273*, 317–323. [[CrossRef](#)]
25. Yan, P.; Yang, F.; Xiang, M.; Wu, T.; Fu, Q. New insights into the memory effect on the crystallization behavior of poly(phenylene sulfide). *Polymer* **2020**, *195*, 122439. [[CrossRef](#)]
26. Somer, A.; Galovic, S.; Lenzi, E.K.; Novatski, A.; Djordjevic, K. Temperature profile and thermal piston component of photoacoustic response calculated by the fractional dual-phase-lag heat conduction theory. *Int. J. Heat Mass Transf.* **2023**, *2023*, 123801. [[CrossRef](#)]
27. Lenzi, E.K.; Somer, A.; Zola, R.S.; da Silva, L.R.; Lenzi, M.K. A Generalized Diffusion Equation: Solutions and Anomalous Diffusion. *Fluids* **2023**, *8*, 34. [[CrossRef](#)]
28. Galovic, S.; Djordjevic, A.I.; Kovacevic, B.Z.; Djordjevic, K.L.; Chevizovich, D. Influence of Local Thermodynamic Non-Equilibrium to Photothermally Induced Acoustic Response of Complex Systems. *Fractal Fract.* **2024**, *8*, 399. [[CrossRef](#)]
29. Hristov, J. Bio-Heat Models Revisited: Concepts, Derivations, Nondimensionalization and Fractionalization Approaches. *Front. Phys.* **2019**, *7*, 189. [[CrossRef](#)]
30. Long, Y.; Shanks, R.A.; Stahurski, Z.H. Kinetics of polymer crystallization. *Prog. Polym. Sci.* **1995**, *20*, 651–701. [[CrossRef](#)]
31. Ziabicki, A. Kinetics of polymer crystallization and molecular orientation in the course of melt spinning. *Appl. Polym. Symp.* **1967**, *6*, 1–18.
32. Malkin, A.Y.; Beghishev, V.P.; Keapin, I.A. Macrokinetics of polymer crystallization. *Polymer* **1983**, *24*, 81–84. [[CrossRef](#)]
33. Mucha, M.; Tylman, M.; Mucha, J. Crystallization kinetics of polycaprolactamin nanocomposites. *Polimery* **2015**, *60*, 686–692. [[CrossRef](#)]
34. Gough, T.E.; Rowat, T.E.; Illner, R. Modeling the solid state reaction $\text{CO}_2 \cdot \text{C}_2\text{H}_2 \rightarrow \text{CO}_2 + \text{C}_2\text{H}_2$. *Chem. Phys. Lett.* **1998**, *298*, 196–200. [[CrossRef](#)]
35. Yang, J.; Grey, K.; Doney, J. An improved kinetic approach to describe the physical stability of amorphous solid dispersions. *Int. J. Pharm.* **2010**, *384*, 24–31. [[CrossRef](#)] [[PubMed](#)]
36. Metin, S.; Hartel, R.W. Thermal analysis of isothermal crystallization kinetics in blends of cocoa butter with milk fat or milk fat fractions. *J. Am. Oil Chem. Soc.* **1998**, *75*, 1617–1624. [[CrossRef](#)]
37. Foubert, I.; Dewettinck, K.; Vanrollghem, P.A. Modelling of the crystallization of fats. *Trends Food Sci. Technol.* **2003**, *14*, 79–92. [[CrossRef](#)]
38. Khanna, Y.P.; Taylor, T.J. Comments and recommendations on the use of the Avrami equation for physico-chemical kinetics. *Polym. Eng. Sci.* **1988**, *28*, 1042–1045. [[CrossRef](#)]
39. Marangoni, A.G. On the use and misuse of the Avrami equation in characterization of the kinetics of fat crystallization. *JAOC* **1998**, *75*, 1465–1467. [[CrossRef](#)]
40. Gorenflo, R.; Kilbas, A.A.; Mainardi, F.; Rogiosin, S.V. *Mittag-Leffler Functions, Related Topics and Applications*; Springer: Berlin/Heidelberg, Germany, 2014.
41. Hilfer, R. Fractional Time evolution. In *Applications of Fractional Calculus in Physics*; Hilfer, R., Ed.; World Scientific: Singapore, 2000; pp. 89–116.
42. Haubold, H.J.; Mathai, A.M. The fractional kinetic equation and thermonuclear functions. *Astrphys. Space Sci.* **2000**, *273*, 53–63. [1002695807970](#). [[CrossRef](#)]
43. Podlubny, I. *Fractional Differential Equations*, 1st ed.; Academic Press: San Diego, CA, USA, 1999.
44. Hristov, J. Non-local kinetics: Revisiting and updates emphasizing fractional calculus applications. *Symmetry* **2023**, *15*, 632. [[CrossRef](#)]
45. Foubert, I.; Vanrollghem, P.A.; Dewettinck, K. Insight in model parameters by studying temperature influence on isothermal cocoa butter crystallization. *Eur. J. Lipid. Sci. Technol.* **2005**, *107*, 660–672. [[CrossRef](#)]

46. Podlubny, I.; Petras, I.; Skovranek, T. Fitting experimental data using Mittag-Leffler function. In Proceedings of the 13th International Carpathian Control Conference (ICCC), High Tatras, Slovakia, 28–31 May 2012; pp. 578–581. [[CrossRef](#)]
47. Fang, C.; Sub, H.; Gu, J. Powell's method-based nonlinear least-square data fitting for the Mittag-Leffler relaxation function. *Math. Mech. Solids* **2017**, *22*, 1058–1067. [[CrossRef](#)]
48. Skovranek, T. The Mittag-Leffler Fitting of the Phillips Curve. *Mathematics* **2019**, *7*, 589. [[CrossRef](#)]
49. Ryapolov, P.A.; Postnikov, E.B. Mittag-Leffler Function as an Approximant to the Concentrated Ferrofluid's Magnetization Curve. *Fractal Fract.* **2021**, *5*, 147. [[CrossRef](#)]
50. Mainardi, F. On some properties of the Mittag-Leffler function $E_\alpha(-t^\alpha)$, complete monotone for $t > 0$ with $0 < \alpha < 1$. *Discret. Contin. Dyn. Syst.-Ser. B* **2014**, *19*, 2267–2278. [[CrossRef](#)]
51. Concezzi, M.; Spigler, R. Some analytical and numerical properties of the Mittag-Leffler functions. *Frac. Calc. Appl. Anal.* **2015**, *18*, 64–94. [[CrossRef](#)]
52. Diethelm, K.; Ford, N.J.; Freed, A.D. Detailed error analysis for a fractional Adams method. *Numer. Algorithms* **2004**, *1*, 31–52.:NUMA.0000027736.85078.be. [[CrossRef](#)]
53. Gorenflo, R.; Loutchko, J.; Luchko, Y. Computation of the Mittag-Leffler function and its derivatives. *Frac. Calc. Appl. Anal.* **2002**, *5*, 491–518.
54. Seybold, H.J.; Hilfer, R. Numerical algorithm for calculating the generalized Mittag-Leffler function. *SIAM J. Numer. Anal.* **2008**, 69–88. [[CrossRef](#)]
55. Valerio, D.; Machado, J.A.T. On the numerical computation of the Mittag-Leffler function. *Commun. Nonlinear Sci. Numer. Simul.* **2014**, *19*, 3419–3424. [[CrossRef](#)]
56. Garrappa, R.; Popolizio, M. Evaluation of generalized Mittag-Leffler functions on the real line. *Adv. Comp. Math.* **2013**, 205–225. [[CrossRef](#)]
57. Garrappa, R. Numerical evaluation of two and three parameter Mittag-Leffler functions. *SIAM J. Numer. Anal.* **2015**, *53*, 1350–1369. [[CrossRef](#)]
58. Liemert, A.; Kienle, A. Time-fractional wave-diffusion equation in an inhomogeneous half-space. *J. Phys. A: Math. Theor.* **2015**, *48*, 225201. [[CrossRef](#)]
59. Ortigueira, M.D.; Lopes, A.M.; Machado, J.T. On the computation of the Mittag-Leffler function. In Proceedings of the International Conference "Fractional Differentiation and Applications", Novi Sad, Serbia, 18–20 July 2016.

Disclaimer/Publisher's Note: The statements, opinions and data contained in all publications are solely those of the individual author(s) and contributor(s) and not of MDPI and/or the editor(s). MDPI and/or the editor(s) disclaim responsibility for any injury to people or property resulting from any ideas, methods, instructions or products referred to in the content.